

Ion-quantized field interaction in two regimes

This content has been downloaded from IOPscience. Please scroll down to see the full text.

2014 Phys. Scr. 89 125101

(<http://iopscience.iop.org/1402-4896/89/12/125101>)

View [the table of contents for this issue](#), or go to the [journal homepage](#) for more

Download details:

IP Address: 200.23.5.162

This content was downloaded on 02/06/2016 at 19:37

Please note that [terms and conditions apply](#).

Ion-quantized field interaction in two regimes

Arturo Zúñiga-Segundo^{1,3}, Raúl Juárez-Amaro²,
Francisco Soto-Eguibar³ and Héctor M Moya-Cessa³

¹Departamento de Física, Escuela Superior de Física y Matemáticas, IPN Edificio 9 Unidad Profesional 'Adolfo López Mateos', 07738 México D.F., Mexico

²Universidad Tecnológica de la Mixteca, Apdo. Postal 71, 69000 Huajuapán de León, Oax., Mexico

³Instituto Nacional de Astrofísica Óptica y Electrónica Calle Luis Enrique Erro No. 1, Sta. Ma. Tonantzintla, Pue. CP 72840, Mexico

E-mail: hmmc@inaoep.mx

Received 19 May 2014

Accepted for publication 10 September 2014

Published 18 November 2014

Abstract

By taking advantage of the superposition principle inherent to quantum mechanics, we show that it is possible, by interacting a quantized field with a trapped ion, to reach both high intensity and low intensity regimes simultaneously. We use the London operator in order to simplify the Hamiltonians involved in the problem.

Keywords: ion-laser interaction, effective Hamiltonians, phase space distributions

(Some figures may appear in colour only in the online journal)

1. Introduction

Trapped ions are considered among the best candidates to perform quantum information processing [1, 2]. By interacting them with laser beams, they are, compared to other systems such as quantized field, moving mirrors, etc., relatively easy to manipulate. This makes them a very good option for the production of nonclassical states of their vibrational motion [3–8, 10], the reconstruction of quasiprobability distribution functions [11], the production of quantum gates [2], etc.

They are an excellent choice for the production of nonlinear coherent states [12], as Hamiltonians may be engineered to have functions (usually Laguerre polynomials) of the phonon number operator [5, 13]; therefore, exponentials (displacements) of sums of nonlinear creation and annihilation operators may be applied to the vacuum in order to generate them.

The trapping of individual ions also offers a lot of possibilities in spectroscopy [14], in the research of frequency standards [15, 16], in the study of quantum jumps [17], and the engineering of specific Hamiltonians [9], to name some additional applications. To make the ions more stable in the trap, to increase the time of confinement, and also to avoid undesirable random motions, it is required

that the ion be in its vibrational ground state. This can be accomplished by means of the adequate use of lasers; with the help of these lasers, the internal energy levels of the trapped ion can be coupled to their vibrational quantum states in such a way that for a certain detuning, the coupling is equivalent to the Jaynes–Cummings Hamiltonian [18–24].

The light that shines the ions is mostly considered classical; however, the electromagnetic field may also be considered quantized [25, 26]. This consideration clearly makes the problem more complicated but also enriches it. For instance, the superposition principle may then be used to reach several regimes that should otherwise be treated separately, such as the high, medium, and low intensity regimes. By treating the light as a quantized field and by choosing a proper initial wave function for it, these regimes are at hand with a single laser field. In what follows we show how this may be achieved.

2. Ion-quantized-field interaction

We consider the interaction between an ion and an electromagnetic quantum field. The Hamiltonian (in units $\hbar = 1$,

which will be used throughout this paper) for this system is

$$\hat{H} = \omega \hat{a}^\dagger \hat{a} + \nu \hat{b}^\dagger \hat{b} + \frac{\omega_0}{2} \hat{\sigma}_z + \Omega \left[\hat{a}^\dagger \hat{\sigma}_- \exp \left[-i\eta(\hat{b} + \hat{b}^\dagger) + i\omega t \right] + H. C. \right], \quad (1)$$

where ω_0 is the atomic transition frequency, ω is the field frequency, Ω the (real) Rabi frequency, ν the harmonic trapping frequency, and η the Lamb–Dicke parameter. The creation and annihilation vibrational operators are denoted b^\dagger and b , respectively, while the field ones are denoted a^\dagger and a . The σ operators are the usual spin Pauli matrices. If we consider $\delta = \omega_0 - \omega$ and go to the rotating frame at frequency ω , we obtain the interaction Hamiltonian

$$\hat{H}_I = \nu \hat{b}^\dagger \hat{b} + \frac{\delta}{2} \hat{\sigma}_z + \Omega \left[\hat{a}^\dagger \hat{\sigma}_- \exp \left[-i\eta(\hat{b} + \hat{b}^\dagger) \right] + \hat{a} \hat{\sigma}_+ \exp \left[i\eta(\hat{b} + \hat{b}^\dagger) \right] \right]. \quad (2)$$

In order to solve the above Hamiltonian, let us define the London [27, 28] or Susskind–Glogower operator [29],

$$\hat{V} = \frac{1}{\sqrt{\hat{a}^\dagger \hat{a} + 1}} \hat{a} = \sum_{n=0}^{\infty} |n\rangle \langle n+1|. \quad (3)$$

Now we transform the interaction Hamiltonian with

$$\hat{T}_V = \begin{pmatrix} \hat{V} & 0 \\ 0 & 1 \end{pmatrix}, \quad (4)$$

and obtain

$$\hat{H}_I = \hat{T}_V \hat{H}_V \hat{T}_V^\dagger, \quad (5)$$

with

$$\hat{H}_V = \begin{pmatrix} \nu \hat{b}^\dagger \hat{b} + \frac{\delta}{2} & \Omega \sqrt{\hat{a}^\dagger \hat{a}} \exp \left[i\eta(\hat{b} + \hat{b}^\dagger) \right] \\ \Omega \sqrt{\hat{a}^\dagger \hat{a}} \exp \left[-i\eta(\hat{b} + \hat{b}^\dagger) \right] & \nu \hat{b}^\dagger \hat{b} - \frac{\delta}{2} \end{pmatrix}, \quad (6)$$

that in terms of the Pauli matrices is written as

$$\hat{H}_V = \nu \hat{b}^\dagger \hat{b} + \frac{\delta}{2} \hat{\sigma}_z + \Omega \sqrt{\hat{a}^\dagger \hat{a}} \left\{ \hat{\sigma}_- \exp \left[-i\eta(\hat{b} + \hat{b}^\dagger) \right] + \hat{\sigma}_+ \exp \left[i\eta(\hat{b} + \hat{b}^\dagger) \right] \right\}. \quad (7)$$

We can perform the transformation $|\psi(t)\rangle = \hat{R}^\dagger |\tilde{\psi}(t)\rangle$, with

$$\hat{R} = \exp \left(i \hat{b}^\dagger \hat{b} \frac{\pi}{2} \right) \exp \left[\frac{\pi}{4} (\hat{\sigma}_+ - \hat{\sigma}_-) \right] \times \exp \left[-i \frac{\eta}{2} (\hat{b} + \hat{b}^\dagger) \hat{\sigma}_z \right], \quad (8)$$

which can be expressed, with the help of displacement

operator $\hat{D}(\beta) = \exp(\beta \hat{b}^\dagger - \beta^* \hat{b})$, as [30],

$$\hat{R} = \frac{1}{\sqrt{2}} \exp \left(i \hat{b}^\dagger \hat{b} \right) \begin{pmatrix} \hat{D}^\dagger \left(\frac{i\eta}{2} \right) & \hat{D} \left(\frac{i\eta}{2} \right) \\ -\hat{D}^\dagger \left(\frac{i\eta}{2} \right) & \hat{D} \left(\frac{i\eta}{2} \right) \end{pmatrix}, \quad (9)$$

such that $\hat{H}_V = \hat{R} \hat{H}_V \hat{R}^\dagger$

$$\hat{H}_V = \nu \hat{b}^\dagger \hat{b} + \Omega \sqrt{\hat{a}^\dagger \hat{a}} \hat{\sigma}_z + \frac{\nu\eta}{2} (\hat{\sigma}_+ + \hat{\sigma}_-) (\hat{b} + \hat{b}^\dagger) + \frac{\delta}{2} (\hat{\sigma}_+ + \hat{\sigma}_-) + \frac{\nu\eta^2}{4}. \quad (10)$$

Note that the interaction part of the above Hamiltonian is linear in the vibrational creation and annihilation operators, much simpler than the interaction part in equation (7), where all the powers of these operators are implicit in the exponential term.

We will consider now for simplicity the high intensity and low intensity regimes in order to diagonalize the Hamiltonian. We apply the unitary transformations,

$$\hat{U}_1 = \exp \left[\xi_1 (\hat{a}^\dagger \hat{\sigma}_+ - \hat{a} \hat{\sigma}_-) \right], \quad \hat{U}_2 = \exp \left[\xi_2 (\hat{a} \hat{\sigma}_+ - \hat{a}^\dagger \hat{\sigma}_-) \right], \quad (11)$$

to the Hamiltonian (10) and consider the parameters $\xi_1, \xi_2 \ll 1$. Under this assumption, we can remain up to the first order in the expansion

$$e^{\xi \hat{A} \hat{B}} e^{-\xi \hat{A}} = \hat{B} + \xi [\hat{A}, \hat{B}] + \frac{\xi^2}{2!} [\hat{A}, [\hat{A}, \hat{B}]] + \dots \approx \hat{B} + \xi [\hat{A}, \hat{B}]$$

and can define the effective Hamiltonian [31] as $\hat{H}_{eff} = \hat{U}_1 \hat{U}_2 \hat{H}_V \hat{U}_2^\dagger \hat{U}_1^\dagger$, whose explicit expression reduces to

$$\hat{H}_{eff} = \nu \hat{b}^\dagger \hat{b} + \Omega \sqrt{\hat{a}^\dagger \hat{a}} \hat{\sigma}_z + \left[\frac{2\nu^2 \eta^2 \Omega \sqrt{\hat{a}^\dagger \hat{a}}}{4\Omega^2 \hat{a}^\dagger \hat{a} - \nu^2} \right] \left(\hat{b}^\dagger \hat{b} + \frac{1}{2} \right) \hat{\sigma}_z + \left[\frac{\nu\eta\delta\Omega\sqrt{\hat{a}^\dagger \hat{a}}}{4\Omega^2 \hat{a}^\dagger \hat{a} - \nu^2} \right] (\hat{b}^\dagger + \hat{b}) \hat{\sigma}_z + \frac{\delta}{2} (\hat{\sigma}_+ + \hat{\sigma}_-), \quad (12)$$

when

$$\xi_1 = \frac{\eta\nu}{2} \left[\frac{1}{2\Omega\sqrt{\hat{a}^\dagger \hat{a}} + \nu} \right], \quad \xi_2 = \frac{\eta\nu}{2} \left[\frac{1}{2\Omega\sqrt{\hat{a}^\dagger \hat{a}} - \nu} \right]. \quad (13)$$

In the resonant case ($\delta = 0$), the effective Hamiltonian becomes diagonal, and we can solve it in an easy way. We also consider the Lamb–Dicke regime, i.e., $\eta \ll 1$. Now, depending on the intensity of the quantized field $\Omega \langle \sqrt{\hat{a}^\dagger \hat{a}} \rangle$ compared to the trap frequency ν , we can produce different approximations in this problem. However, taking into account the superposition principle in quantum mechanics, we can produce several regimes—simultaneously low, medium, and high intensity regimes—in contrast to the classical field case [10]. If we consider, for instance, an initial field wavefunction

of the form

$$|\psi_F(0)\rangle = C_s |s\rangle + C_m |m\rangle + C_l |l\rangle, \quad (14)$$

where $|s\rangle$, $|m\rangle$, and $|l\rangle$ are number states and their amplitudes satisfy the normalization condition $|C_s|^2 + |C_m|^2 + |C_l|^2 = 1$, the different intensity regimes may be achieved simultaneously, provided that

$$\nu \ll \Omega\sqrt{l}, \quad \text{HIR} \quad (15)$$

$$\nu \approx 2\Omega\sqrt{m}, \quad \text{MIR} \quad (16)$$

$$\nu \gg \Omega\sqrt{s}, \quad \text{LIR} \quad (17)$$

For simplicity, we will consider $C_m = 0$ as we study the high and low intensity regimes simultaneously. We assume the total initial state as

$$|\psi(0)\rangle = |g\rangle |\psi_V(0)\rangle |\psi_F(0)\rangle, \quad (18)$$

where the vibrational wavefunction $|\psi_V(0)\rangle = |\alpha\rangle$ is a coherent state, and α is a real number, to avoid extra phases (although the calculation may be done for complex α).

Then the solutions to the Schrödinger equation for the interaction Hamiltonian reads

$$\begin{aligned} |\psi(t)\rangle &= e^{-i\hat{H}_I t} |\psi(0)\rangle, \\ &= \left[C_s \hat{T}_V \hat{R}^\dagger e^{-i\hat{H}_{eff} \hat{R}} |s\rangle + C_l \hat{T}_V \hat{R}^\dagger e^{-i\hat{H}_{eff} \hat{R}} |l\rangle \right] |g\rangle |\alpha\rangle, \\ &= \frac{C_s}{2} \begin{bmatrix} |\psi_e^s(t)\rangle |s-1\rangle \\ |\psi_g^s(t)\rangle |s\rangle \end{bmatrix} + \frac{C_l}{2} \begin{bmatrix} |\psi_e^l(t)\rangle |l-1\rangle \\ |\psi_g^l(t)\rangle |l\rangle \end{bmatrix}, \end{aligned} \quad (19)$$

where the kets $|\psi_e^k(t)\rangle$ and $|\psi_g^k(t)\rangle$ are given by

$$\begin{aligned} |\psi_e^k(t)\rangle &= \left| \frac{i\eta}{2} + i\beta_e^k \right\rangle \exp \left[i(\phi_e^k - \phi_t^k) \right] \\ &\quad - \left| \frac{i\eta}{2} + i\beta_g^k \right\rangle \exp \left[i(\phi_g^k + \phi_t^k) \right], \end{aligned} \quad (20)$$

$$\begin{aligned} |\psi_g^k(t)\rangle &= \left| -\frac{i\eta}{2} + i\beta_e^k \right\rangle \exp \left[-i(\phi_e^k + \phi_t^k) \right] \\ &\quad + \left| -\frac{i\eta}{2} + i\beta_g^k \right\rangle \exp \left[-i(\phi_g^k - \phi_t^k) \right], \end{aligned} \quad (21)$$

with $k = s, l$. We have defined

$$\begin{aligned} \beta_e^k &= \left(\frac{\eta}{2} + \alpha \right) \exp(-it\omega_e^k), \\ \beta_g^k &= \left(\frac{\eta}{2} + \alpha \right) \exp(-it\omega_g^k), \end{aligned} \quad (22)$$

$$\phi_e^k = \frac{\eta}{2} \left(\frac{\eta}{2} + \alpha \right) \sin \omega_e^k t, \quad \phi_g^k = \frac{\eta}{2} \left(\frac{\eta}{2} + \alpha \right) \sin \omega_g^k t, \quad (23)$$

$$\omega_e^k = \nu + 2g(k), \quad \omega_g^k = \nu - 2g(k), \quad (24)$$

$$\phi^k = \Omega\sqrt{k} + g(k), \quad g(k) = (\eta^2 \nu^2 \Omega \sqrt{k}) (4\Omega^2 k - \nu^2)^{-1}. \quad (25)$$

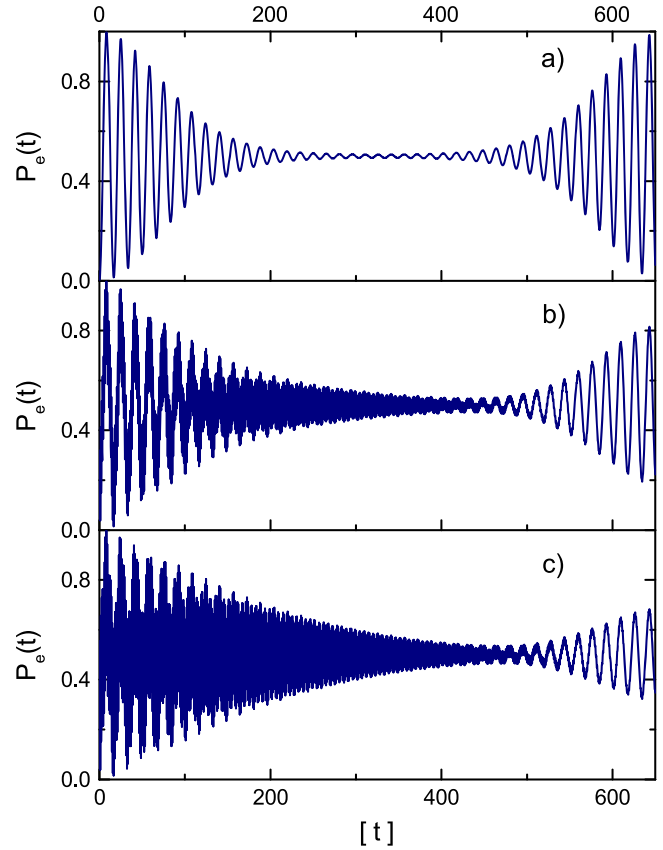


Figure 1. Time evolution of the probability to find the ion in its excited state $P_e(t)$ for $\eta = 0.1$, $\Omega = 0.2$, and $\nu = 1.0$. We assumed an initial field wavefunction superposition with $s = 1$ and $l = 200$ as $|\psi_F(0)\rangle = \sqrt{1-r^2}|1\rangle + r|200\rangle$, with (a) $r = 0$, (b) $r = 0.6$ and (c) $r = 0.8$. The initial vibrational wavefunction was the coherent state $|\psi_V(0)\rangle = |\alpha\rangle$ with $\alpha = 2.0$. The ion was considered initially in its ground state.

3. System dynamics

With the time evolved wavefunction given in equation (19), we can calculate the probability to find the ion in its excited state $P_e(t)$ as a function of time and the Wigner function for the vibrational states, which can be written as

$$\begin{aligned} W(\gamma) &= \frac{|C_s|^2}{4} [W_e^s(\gamma) + W_g^s(\gamma)] \\ &\quad + \frac{|C_l|^2}{4} [W_e^l(\gamma) + W_g^l(\gamma)], \end{aligned} \quad (26)$$

where

$$W_{e,g}^k(\gamma) = \frac{1}{\pi} \sum_{m=0}^{\infty} (-1)^m \left| \langle m | \hat{D}^\dagger(\gamma) | \psi_{e,g}^k(t) \rangle \right|^2, \quad (27)$$

with $k = s, l$ and $\gamma = (q + ip)/\sqrt{2}$ a point in phase space. For all the plots, the initial conditions have been chosen with the coherence parameter $\alpha = 2.0$; we fixed parameters $\eta = 0.1$, $\Omega = 0.2$, and $\nu = 1.0$. We analyze the effects resulting from variation of the coefficients C_s and C_l on $P_e(t)$ and $W(\gamma)$. For

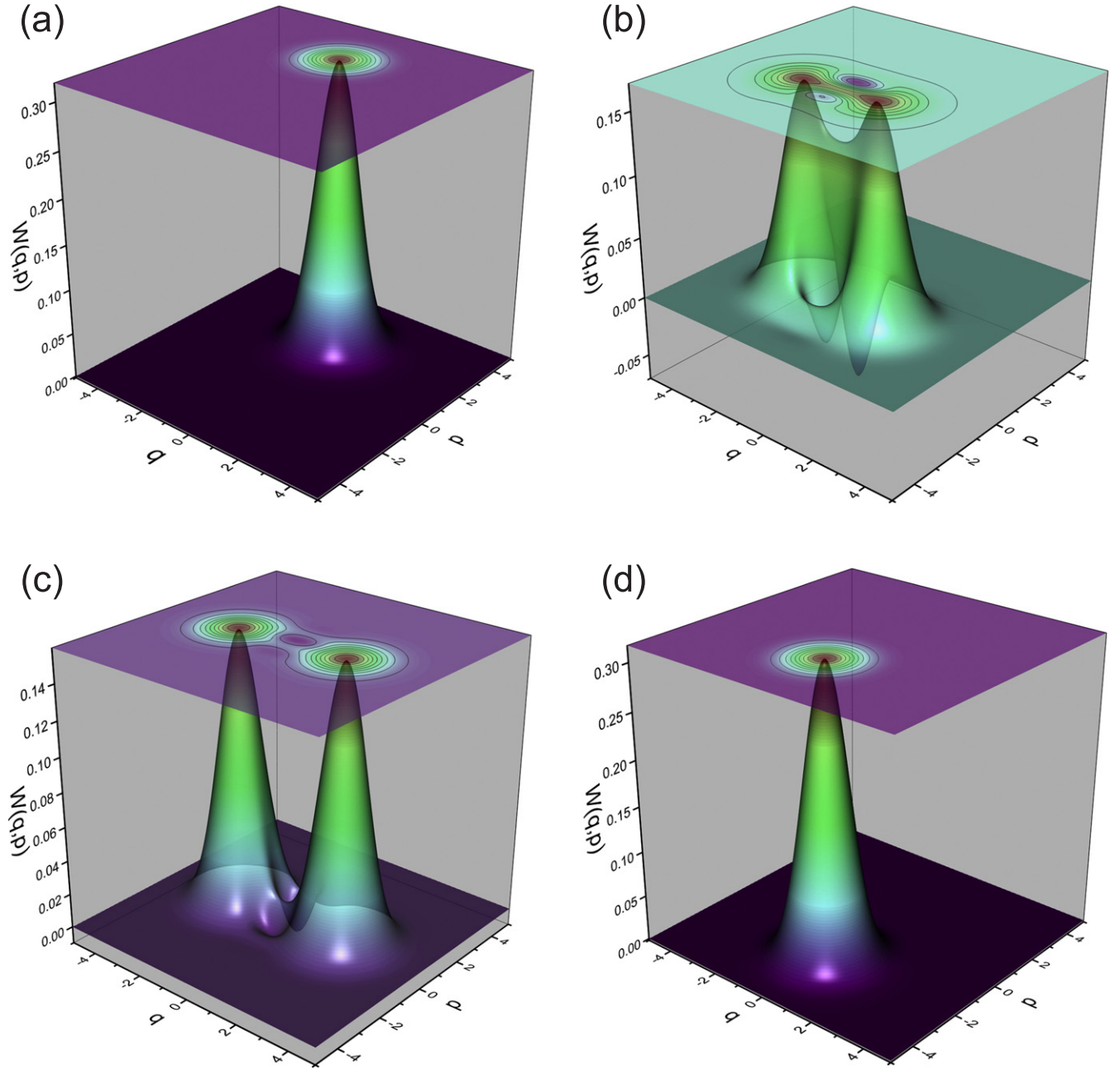


Figure 2. Time evolution of the Wigner function for the vibrational states of the ion for: (a) $t = 0$, (b) $t = 172.78$, (c) $t = 345.57$, and (d) $t = 659.70$. We assumed an initial field wavefunction in a superposition of number states, with $s = 1$ and $l = 200$, as $|\psi_F(0)\rangle = \sqrt{1 - r^2}|1\rangle + r|200\rangle$, with $r = 0$. The initial vibrational wavefunction was the coherent state $|\psi_V(0)\rangle = |\alpha\rangle$ with $\alpha = 2.0$, and the ion was considered initially in its ground state. $\eta = 0.1$, $\Omega = 0.2$, and $\nu = 1.0$ as in figure 1.

the sake of simplicity, we are going to consider $C_s = \sqrt{1 - r^2}$ and $C_l = r$, where r allows one to control the corresponding coefficients of the superposition. In our computations, we have also chosen the initial field wavefunction superposition for $s = 1$ and $l = 200$ as

$$|\psi_F(0)\rangle = \sqrt{1 - r^2}|1\rangle + r|200\rangle \quad (28)$$

in order to satisfy the high and low intensity regimes at the same time, which are defined by equations (15) and (17), respectively.

Figure 1 displays the evolution of the atomic level occupation probability of the upper level $P_e(t)$ for different values of r . It is worth mentioning that $P_e(t)$ evolves periodically, and their oscillations exhibit ‘collapse-revival’ behaviour. In figure 1(a) we plot $P_e(t)$ when the parameter $r = 0$; i.e., in this case we have only a number state $|1\rangle$ in the field wavefunction. Hence we observe a Rabi oscillation of $\Omega\sqrt{1}$ in the probability $P_e(t)$. When $r = 0.6$, we have two Rabi oscillations in $P_e(t)$, $\Omega\sqrt{1}$, and $\Omega\sqrt{200}$, and this probability becomes spiky. Increasing further $r = 0.8$, large oscillations and spikes in the probability appear (see

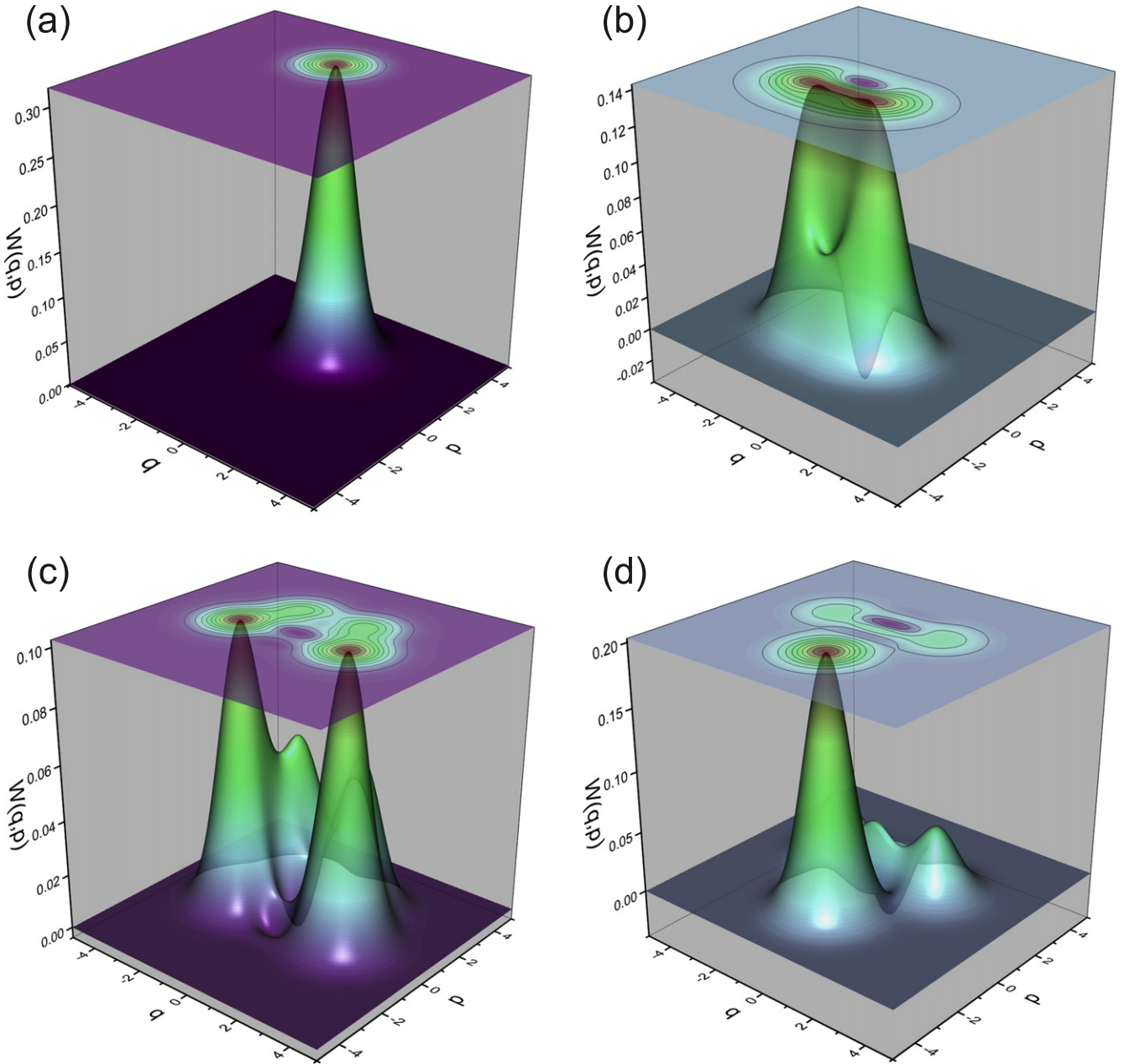


Figure 3. Time evolution of the Wigner function for the vibrational states of the ion for: (a) $t = 0$, (b) $t = 172.78$, (c) $t = 345.57$, and (d) $t = 659.70$. We assumed an initial field wavefunction in a superposition of number states, with $s = 1$ and $l = 200$, as $|\psi_F(0)\rangle = \sqrt{1-r^2}|1\rangle + r|200\rangle$, with $r = 0.6$. The initial vibrational wavefunction was the coherent state $|\psi_V(0)\rangle = |\alpha\rangle$ with $\alpha = 2.0$, and the ion was considered initially in its ground state. $\eta = 0.1$, $\Omega = 0.2$, and $\nu = 1.0$ as in figure 1.

figure 1(c)). When $r = 1$, we have the same effect as in figure 1(a) but with additional peaks and a different period. This is of course due to the increase of the intensity of the quantized field.

In figure 2 we show the time evolution in phase space of the Wigner function for the vibrational states of the ion when $r = 0$. At $t = 0$ (figure 2(a)), the initial Wigner function has the shape of a single hump. With the increase of time, this hump revolving around a circle of radius α will split into two humps, because each one has a slightly different angular velocity (this may be seen from equation (24)), as it is shown

in figure 2(b) when $t \approx 172.78$. The two motional branches of the Wigner function of the field vibration mode determine the oscillatory behaviour of the atomic level occupation probability of figure 1(a) due to the interference between the two humps. In figure 2(b) it may be seen that the Wigner function takes negative values. When $t \approx 345.57$, the humps are well separated (see figure 2(c)), and the Rabi oscillations are small compared with the initial ones (see figure 1(a)); also the negative values of the Wigner function are small too. We have the collapse region when $t > 345.57$, and the collision of two humps leads to the revival of Rabi oscillations, whose

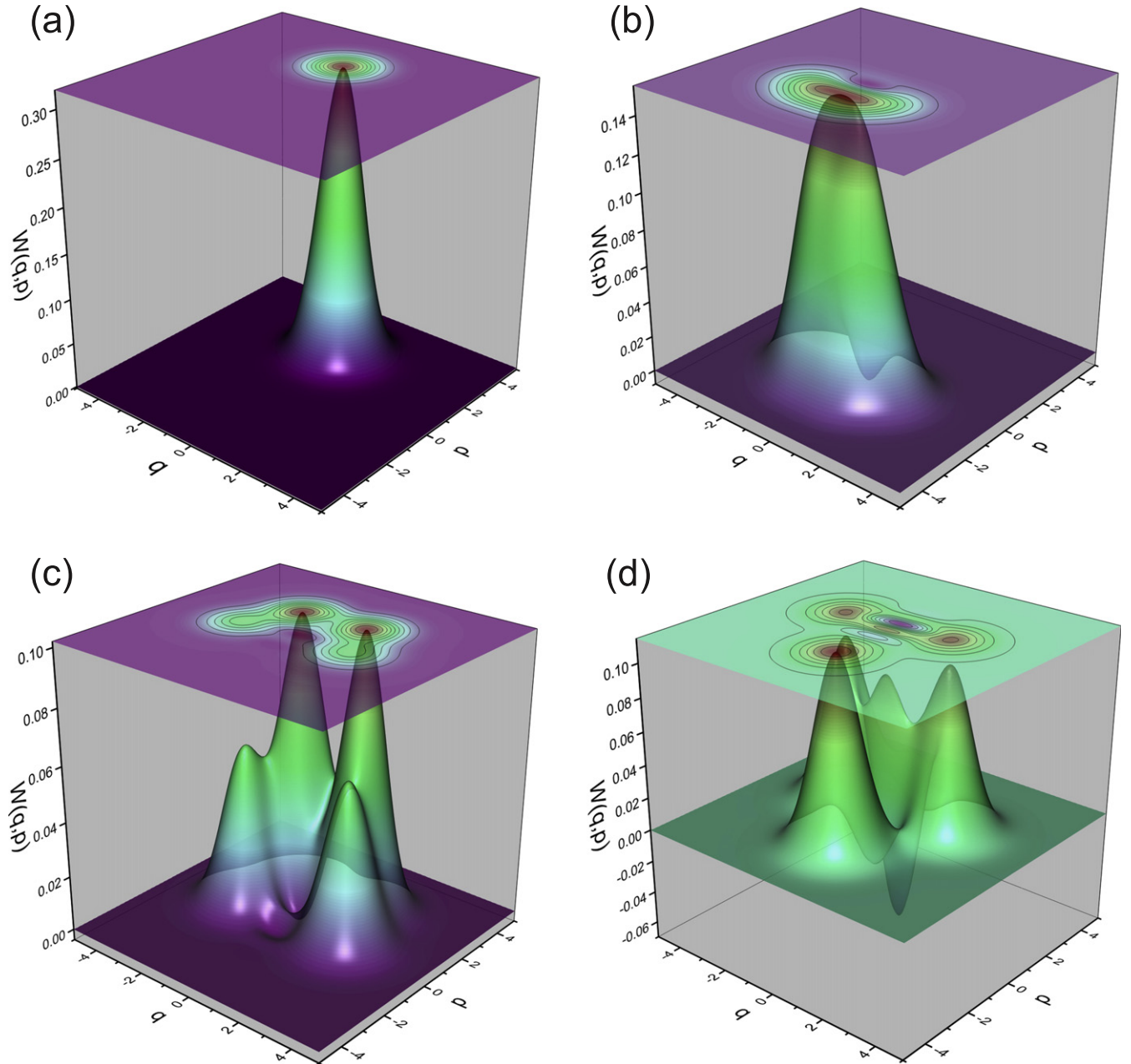


Figure 4. Time evolution of the Wigner function for the vibrational states of the ion for: (a) $t = 0$, (b) $t = 172.78$, (c) $t = 345.57$, and (d) $t = 659.70$. We assumed an initial field with $s = 1$ and $l = 200$, as $|\psi_F(0)\rangle = \sqrt{1-r^2}|1\rangle + r|200\rangle$, with $r = 0.8$. The initial vibrational wavefunction was the coherent state $|\psi_V(0)\rangle = |\alpha\rangle$ with $\alpha = 2.0$, and the ion was considered initially in its ground state. $\eta = 0.1$, $\Omega = 0.2$, and $\nu = 1.0$ as in figure 1.

maximum value it reaches when we recover the initial hump at time $t \approx 659.70$, as shown in figure 2(d).

A similar behaviour for Wigner functions occurs when $r = 0.6$, as shown in figure 3. In order to compare it with results shown in the previous figure, we have considered the same interaction times in each of figures 3(a)–(d) and 4(a)–(d). At $t = 0$ we have a single hump (see figure 3(a)); as time goes on, it splits into two humps, as shown in figure 3(b). These humps will not be well separated; in this case, the humps are spread on the circle of radius α as in figure 3(c). Finally, we cannot recover the initial Wigner function at $t \approx 659.70$, as shown in figure 3(d), where two new humps

appear due to the different frequencies that arise because of the high and low intensity regimes. The heights and widths of these new humps can be increased by setting $r = 0.8$, as shown in figure 4(d). Also, figure 4(c) shows how the Wigner function is spread on the circular path before it splits up.

4. Conclusions

We have taken advantage of the use of the London–Susskind–Glogower operator to transform the ion–laser–quantized field

Hamiltonian in an easy form. We considered an initial superposition of number states in the field wavefunction in order to study simultaneously the high and low intensity regimes. This revealed a behaviour of the Wigner function of the vibrational motion not observed when a classical field is considered.

References

- [1] Cirac J I and Zoller P 1995 *Phys. Rev. Lett.* **74** 4091
- [2] Jonathan D, Plenio M B and Knight P L 2000 *Phys. Rev. A* **62** 042307
- [3] Meekhof D M, Monroe C, King B E, Itano W M and Wineland D J 1996 *Phys. Rev. Lett.* **76** 1796
- [4] Wallentowitz S and Vogel W 1997 *Phys. Rev. A* **55** 4438
- [5] Wallentowitz S, Vogel W and Knight P L 1999 *Phys. Rev. A* **59** 531
- [6] Kis Z, Vogel W and Davidovich L 2001 *Phys. Rev. A* **64** 033401
- [7] de Matos Filho R L and Vogel W 1996 *Phys. Rev. Lett.* **76** 608
- [8] de Matos Filho R L and Vogel W 1996 *Phys. Rev. A* **54** 4560
- [9] de Matos Filho R L and Vogel W 1998 *Phys. Rev. A* **58** R1661
- [10] Moya-Cessa H M, Soto-Eguibar F, Vargas-Martinez J M, Juarez-Amaro R and Zúñiga-Segundo A 2012 *Phys. Rep.* **513** 229
- [11] Leibfried D, Meekhof D, King B E, Monroe C, Itano W M and Wineland D J 1996 *Phys. Rev. Lett.* **77** 4281
- [12] Man'ko V I, Marmo G, Sudarshan E C G and Zaccaria F 1997 *Phys. Scr.* **55** 528
- [13] Moya-Cessa H and Tombesi P 2000 *Phys. Rev. A* **61** 025401
- [14] Itano W M, Bergquist J C, Hulet R G and Wineland D J 1988 *Phys. Scr.* **T22** 79
- [15] Wineland D J, Bollinger J J, Itano W M, Moore F L and Heinzen D J 1992 *Phys. Rev. A* **46** R6797
- [16] Bollinger J J, Prestage J D, Itano W M and Wineland D J 1985 *Phys. Rev. Lett.* **54** 1000
- [17] Powell H F, van Eijkelenborg M A, Irvine I, Segal D M and Thompson R C 2002 *J. Phys. B: At. Mol. Opt. Phys.* **35** 205
- [18] Jaynes E T and Cummings F W 1963 *Proc. IEEE* **51** 89
- [19] Paul H 1963 *Ann. Phys. (Lpz.)* **11** 411
- [20] Blockley C A, Walls D F and Risken H 1992 *Europhys. Lett.* **17** 509
- [21] Agarwal G S 1987 *J. Mod. Opt.* **34** 909
- [22] Agarwal G S and Kumar S A 1991 *Phys. Rev. Lett.* **67** 3665
- [23] Shore B W and Knight P L 1993 *J. Mod. Opt.* **40** 1195
- [24] Cirac J I, Blatt R, Parkins A S and Zoller P 1994 *Phys. Rev. A* **49** 1202
- [25] Zeng H-P and Lin F-C 1994 *Phys. Rev. A* **50** R3589
- [26] Semião F L and Vidiella-Barranco A 2005 *Phys. Rev. A* **71** 065802
- [27] London F 1926 *Z. Phys* **37** 915
- [28] London F 1927 *Z. Phys* **40** 193
- [29] Susskind L and Glogower J 1964 *Physics* **1** 49
- [30] Moya-Cessa H, Jonathan D and Knight P L 2003 *J. Mod. Opt.* **50** 265
- [31] Klimov A B and Sanchez-Soto L L 2000 *Phys. Rev. A* **61** 063802